

Supporting Information

Charge Transfer Alteration and White Light Emission in Photochromic Triphenylamine-Norbornadiene-Triazine Switch

Manoj Upadhyay, Raktim Deka, and Debdas Ray*

Advanced Photofunctional Materials Laboratory, Department of Chemistry, Shiv Nadar Institution of Eminence, Delhi NCR, NH-91, Tehsil Dadri, Gautam Buddha Nagar, Uttar Pradesh, India, 201314.

Email: debdas.ray@snu.edu.in.

Contents

S1. Experimental details.....	3
S2. Synthesis and characterization of the compound.....	3
S3. Preparation of single crystal and SCXRD analysis.....	6
S4. Absorption and photoisomerization studies.....	7
S5. Kinetic studies of the thermal back conversion	11
S6. Photoluminescence (PL) studies	13
S7. Quantum studies.....	15
S8. Supporting references	21

S1. Experimental details

General information. All the reagents and deuterated solvents were obtained from commercial sources and used without further purification unless otherwise mentioned. Synthesised compounds were purified by column chromatography using silica gel (Acytilis, 60 Å, 230-400 mesh) as stationary phase, and solvent mixtures used during chromatography were reported as volume ratios unless otherwise noted. Deuterated solvents were purchased from Eurisotop (Cambridge Isotope Laboratories, Inc.) and used as received. Spectroscopic grade solvents were used for the spectroscopic measurements. Photoisomerization was performed using Kessil LED PR160L -390 nm and PR160L-427 nm.

Characterization. ^1H and ^{13}C NMR spectra were recorded in Bruker AVHDN 400 with working frequencies of 400.2 MHz for ^1H and 100.6 MHz for ^{13}C nuclei, respectively. Chemical shifts are quoted in ppm relative to tetramethylsilane (TMS), using the residual solvent peak as the reference standard. High-resolution mass Spectroscopy (HRMS) was carried out using an Agilent 6540 accurate mass Q-TOF LC/MS (Agilent Technologies, U.S.A.). Single crystal X-ray diffraction data were collected using a D8 Venture μS microfocus dual source Bruker APEX4 diffractometer equipped with a PHOTON 100 CMOS detector and an Oxford cryogenic system. Single crystals were mounted at room temperature on the ends of glass fibers, and data were collected at room temperature. Data collection: APEX4 (Bruker, 2014)¹ cell refinement: SAINT (Bruker, 2014)¹ data reduction: SAINT; program(s) used to solve structure: OLEX 2 (Olexsys)² program(s) used to refine structure.

Photophysical measurements. UV absorption was measured by Agilent Technologies Cary 8454 UV absorption instrument equipped with Peltier in a conventional quartz cell cuvette or Cary 100 UV absorption instrument. Steady-state emission spectra were recorded on an Edinburgh Instruments spectrophotometer equipped with standard cuvette holder SC-05 (Model: FS5) fitted with a PMT-900 detector and excited with a 150W CW Ozone-free xenon arc lamp.³ Absolute photoluminescence quantum yield was measured using integration sphere module SC-30 supplied by Edinburgh Instruments. All other measurement techniques were discussed in earlier reports.³

S2. Synthesis and characterization of the compound

4-(3-(4-(4,6-diphenyl-1,3,5-triazin-2-yl)phenyl)bicyclo[2.2.1]hepta-2,5-dien-2-yl)-N,N-diphenylaniline (TPNTZ). TPNTZ was synthesized through a one-pot Suzuki coupling reaction under an inert atmosphere. In an oven-dried, double-neck, 50 mL round-bottom flask, equimolar amounts of (4-(diphenylamino)phenyl)boronic acid (0.23 g, 0.80 mmol) and 2,4-

diphenyl-6-(4-(4,4,5,5-tetramethyl-1,3,2-dioxaborolan-2-yl)phenyl)-1,3,5-triazine (0.35 g, 0.80 mmol) were combined. Caesium fluoride (0.73 g, 4.8 mmol) and a catalytic amount of $\text{Pd}_2(\text{dba})_3$ (0.05 mol%) were added. The flask was evacuated and filled with argon three times to maintain an inert environment. A small quantity of tri-tert-butylphosphonium tetrafluoroborate (0.03 g) and 10 mL of anhydrous tetrahydrofuran were introduced, and the mixture was purged again with argon. Finally, 2,3-dibromonorbornadiene (0.2 g, 0.80 mmol) was added. The reaction was stirred at room temperature for 24 hours. Upon completion, the mixture was quenched with cold water, and the organic compounds were extracted with dichloromethane. The combined organic layers were washed with brine and dried over sodium sulphate. The crude product was purified by silica gel chromatography using hexane. **TPNTZ** was isolated as a yellow solid in 53% yield (0.32 g). ^1H NMR (400 MHz, CD_2Cl_2) δ (ppm): 8.77 (d, $J = 7.3$ Hz, 4H), 8.67 (d, $J = 8.3$ Hz, 2H), 7.65 – 7.57 (m, 6H), 7.51 (d, $J = 8.3$ Hz, 2H), 7.26 (t, $J = 7.8$ Hz, 4H), 7.19 (d, $J = 8.5$ Hz, 2H), 7.12 – 6.99 (m, 8H), 6.95 (d, $J = 8.5$ Hz, 2H), 3.96 (d, $J = 15.9$ Hz, 2H), 2.39 (d, $J = 6.1$ Hz, 1H), 2.11 (d, $J = 6.1$ Hz, 1H). ^{13}C NMR (101 MHz, CD_2Cl_2) δ (ppm): 172.06, 171.87, 151.34, 148.10, 147.34, 143.17, 143.12, 142.86, 136.86, 134.64, 133.05, 131.85, 129.80, 129.39, 129.19, 128.42, 127.72, 125.27, 125.05, 123.56, 123.52, 70.57, 57.48, 57.30, 54.00. HRMS(ESI) m/z : calcd. for $\text{C}_{46}\text{H}_{34}\text{N}_4$ $[\text{M}+\text{H}]^+$ 643.2876, found, 643.2956.

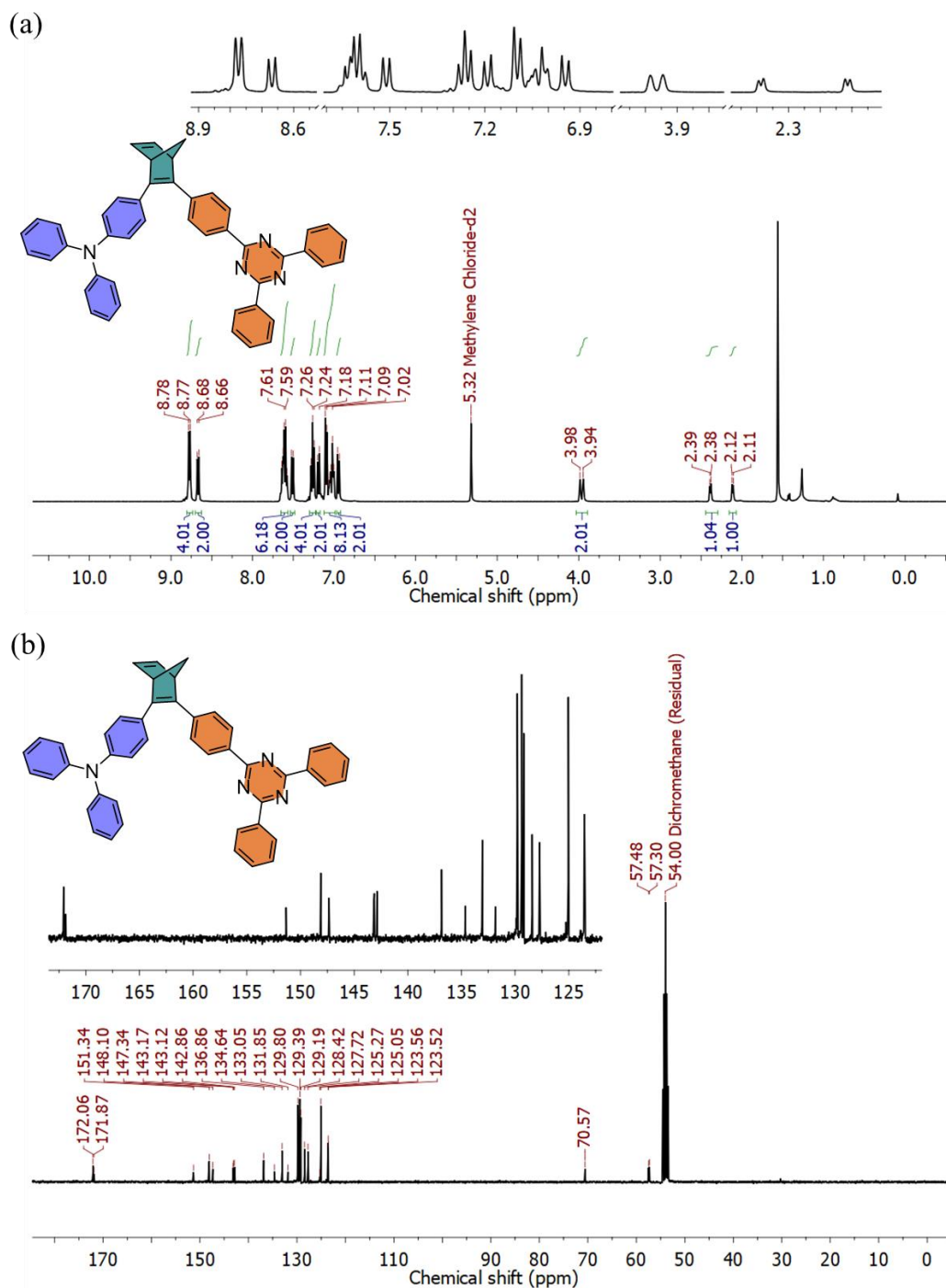


Fig. S1. (a) ^1H (400.2 MHz, CD_2Cl_2) and (b) ^{13}C NMR (100.6 MHz, CD_2Cl_2) spectra of 4-3-(4-(4,6-diphenyl-1,3,5-triazin-2-yl)phenyl)bicyclo[2.2.1]hepta-2,5-dien-2-yl)-N,N-diphenylaniline (TPNTZ).

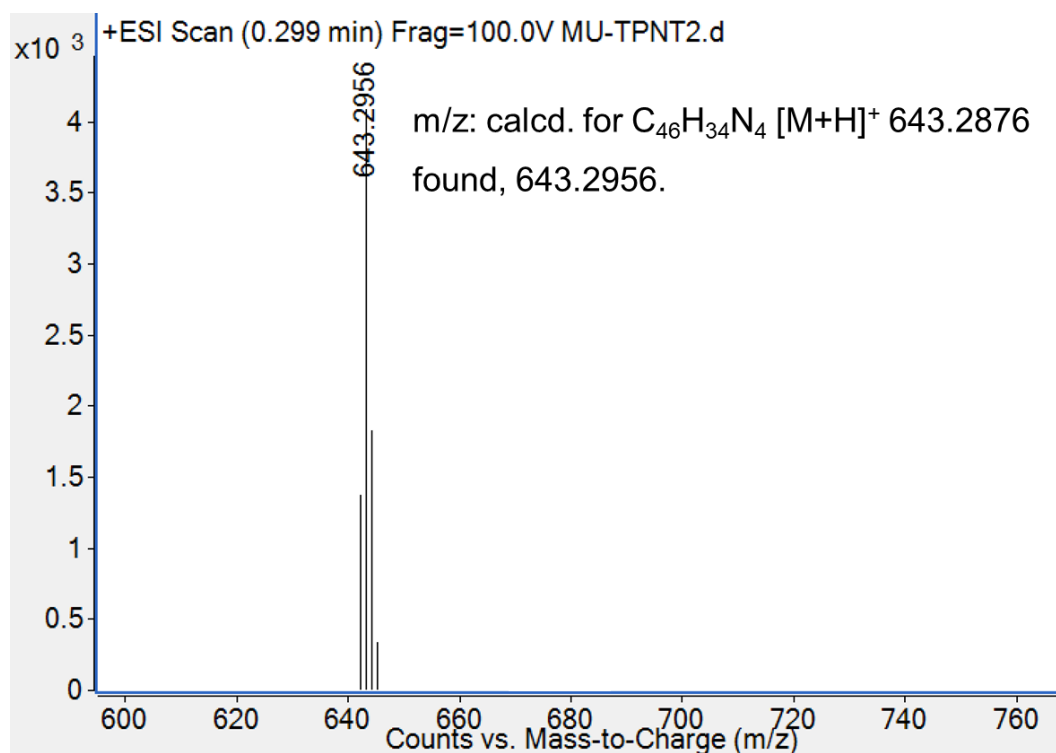


Fig. S2. Mass spectrogram of **TPNTZ**.

S3. Preparation of single crystal and SCXRD analysis

Preparation of the **TPNTZ** crystal: **TPNTZ** (10.0 mg) was dissolved in 1.0 mL of dichloromethane, and the resulting solution was layered with n-hexane (2.0 mL). The solvent was allowed to evaporate to yield block-shaped yellow crystals suitable for X-ray diffraction.

Table S1a. Crystal data and structure refinement for **TPNTZ**

Identification code	TPNTZ
CCDC	2441493
Empirical formula	$\text{C}_{46}\text{H}_{35}\text{N}_4$
Formula weight	643.78
Temperature/K	277.00
Crystal system	monoclinic
Space group	C2/c
a/Å	34.526(6)
b/Å	6.0518(11)
c/Å	34.924(7)
$\alpha/^\circ$	90
$\beta/^\circ$	91.885(5)
$\gamma/^\circ$	90
Volume/Å ³	7293(2)
Z	8
$\rho_{\text{calc}}/\text{g cm}^{-3}$	1.173

μ/mm^{-1}	0.069
F(000)	2712.0
Crystal size/ mm^3	$0.21 \times 0.17 \times 0.16$
Radiation	MoK α ($\lambda = 0.71073$)
2 Θ range for data collection/ $^\circ$	4.668 to 54.366
Index ranges	$-44 \leq h \leq 43$, $-7 \leq k \leq 7$, $-44 \leq l \leq 44$
Reflections collected	41756
Independent reflections	7801 [$R_{\text{int}} = 0.0825$, $R_{\text{sigma}} = 0.0566$]
Data/restraints/parameters	7801/0/453
Goodness-of-fit on F^2	0.943
Final R indexes [$I \geq 2\sigma(I)$]	$R_1 = 0.0899$, $wR_2 = 0.2512$
Final R indexes [all data]	$R_1 = 0.1782$, $wR_2 = 0.3655$
Largest diff. peak/hole / $e \text{ \AA}^{-3}$	0.33/-0.27

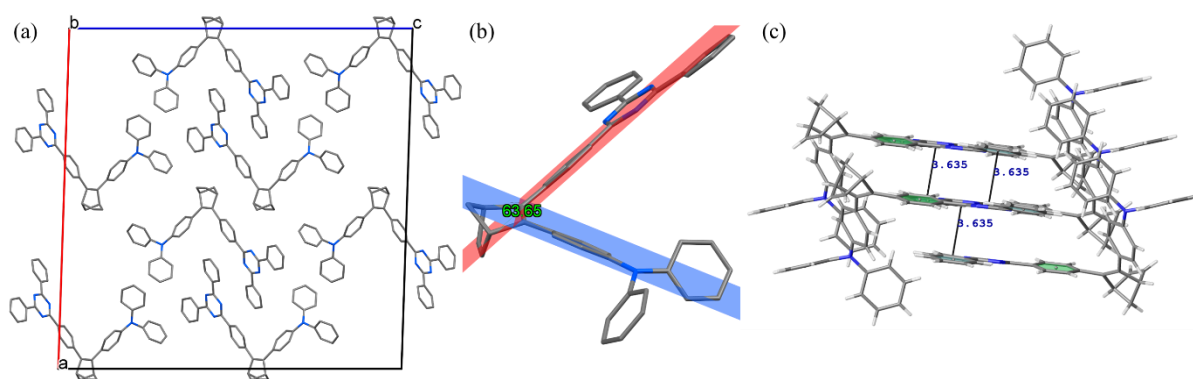


Fig. S3. (a) Unit cell viewed along b – axis, (b) angles passing through phenyl- groups of TPA and TNZ, and (c) intermolecular interactions showing the distance between triazine rings and adjacent phenyl rings of TPNTZ.

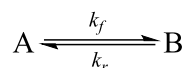
S4. Absorption and photoisomerization studies

Photoisomerization quantum yields: The molar photon flux I_0 of the light source (Xenon lamp of Edinburgh Instruments spectrophotometer FS5) at 310 and 427 nm were determined using chemical actinometry.⁴ A 0.002 L ($= V_0$) solution of potassium ferrioxalate in 0.05 M H_2SO_4 was placed into a 1.0 cm cuvette and irradiated for 30 seconds ($= t_0$). The irradiated solution was combined with 0.001 L phenanthroline (0.1 wt. % in 0.5 M H_2SO_4 /1.6 M NaOAc) and stirred under the dark for an hour. The resulting solution 0.003 L ($= V$), containing reddish-purple $[\text{Fe}(\text{Phen})_3]^{2+}$ complex, was diluted by a factor of n , and its absorbance was measured at 510 nm (A_{510}), where its molar absorption coefficient (ϵ_{510}) is $11,100 \text{ M}^{-1} \text{ cm}^{-1}$. The molar photon flux of the light source at different wavelengths was determined using the following equation.

$$(I_0 \text{ (mol.s}^{-1}\text{)}) = \frac{A_{510} \times n \times V}{t_0 \times l \times \phi_\lambda \times \varepsilon_{510} \times 1000 \times V_0} \quad (\text{S1})$$

where l indicates the length of cuvette; and ϕ_λ stands for the quantum yield of photo reduction of Fe(III)oxalate induced by the light ($\phi_{310} = 1.23$, $\phi_{427} = 1.12$).⁴ The photon flux I_0 (mol. s⁻¹) at 427, and 310 nm (Edinburgh FS5 Spectrofluorometer Xenon lamp) used for the photoisomerization is 3.9×10^{-9} mol s⁻¹ and 2.78×10^{-9} mol s⁻¹ respectively.

The Photoisomerization quantum yield of all the parent and isomers were measured according to the previously reported method.



In a photochemical reaction, species A absorbs light to generate product B. The general kinetics of a basic photochemical reaction can be expressed using equation (S2).

$$\frac{dA}{dt} = \frac{I_0 \cdot \phi_{A \rightarrow B}}{V_A} (1 - 10^{-\varepsilon_A C_A l}) \quad (\text{S2})$$

When $\varepsilon_A \cdot C_A \cdot l \cdot \ln 10 \ll 1$, the Taylor expansion can be expressed as first order term, simplifying the equation.

$$k_{A \rightarrow B} = \frac{I_0 \cdot \phi_{A \rightarrow B}}{V_A} \varepsilon_A \cdot l \cdot \ln 10 \quad (\text{S3})$$

Rearranging the above equation for $\phi_{A \rightarrow B}$ calculation,

$$\phi_{A \rightarrow B} = \frac{k_{A \rightarrow B} \cdot V_A}{I_0 \cdot \varepsilon_A \cdot l \cdot \ln 10} \quad (\text{S4})$$

Where $\phi_{A \rightarrow B}$ represents photoisomerization yield from A to B; $k_{A \rightarrow B}$ indicates rate constant (obtained by the exponential fitting of a graph of Abs. vs Time); V_A is sample volume; I_0 indicates molar photon flux; ε_A is molar absorption coefficient of sample A; and l is light path length.

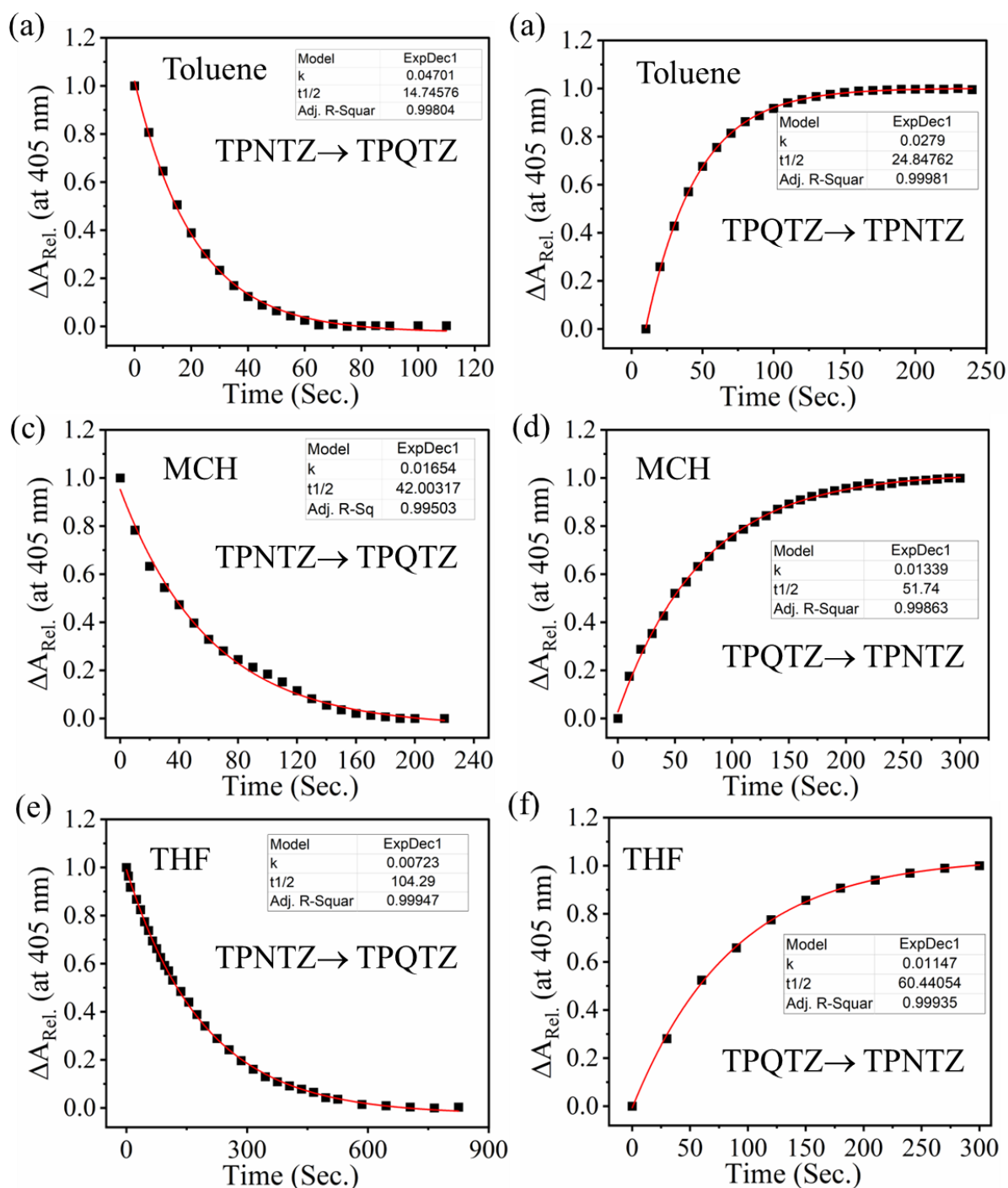
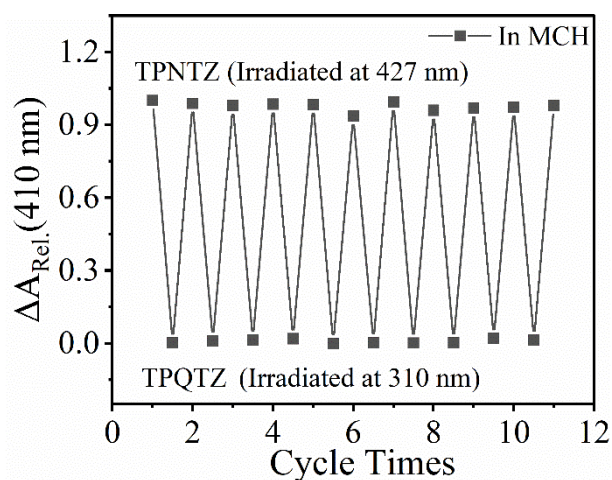
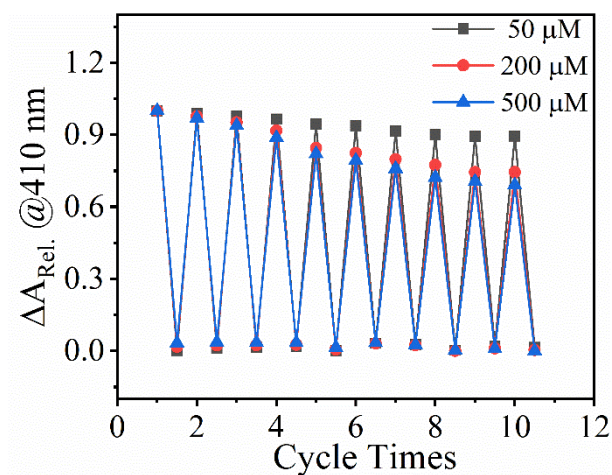


Fig. S4. Kinetics plot showing reversible photoisomerization in various solvents (a) TPNTZ \rightarrow TPQ TZ in toluene, (b) TPQ TZ \rightarrow TPNTZ in toluene, (c) TPNTZ \rightarrow TPQ TZ in MCH, (d) TPQ TZ \rightarrow TPNTZ in MCH, (e) TPNTZ \rightarrow TPQ TZ in THF, (f) TPQ TZ \rightarrow TPNTZ in THF.

Table S2. Reversible photoisomerization Quantum yields (ϕ) in different solvents.

Photochemical process*	Toluene	MCH	THF
$\phi_{TPNTZ \rightarrow TPQTZ}$ at 427 nm	$66.64 \pm 1.8 \%$	$25.04 \pm 1.5 \%$	$10.49 \pm 1.0 \%$
$\phi_{TPQTZ \rightarrow TPNTZ}$ at 310 nm	$55.20 \pm 2.0 \%$;	$23.5 \pm 1.5 \%$	$22.7 \pm 1.3 \%$
* $\epsilon_{TPNTZ} = 23684 \text{ M}^{-1} \text{ cm}^{-1}$, Path length (l) = 1 cm, Concentration (V) = 0.003 L			

**Fig. S5.** Two-way reversible photoswitching in MCH (conc. = 10 μM).**Fig. S6.** Concentration-dependent two-way photoswitching showing photo-degradation in toluene.

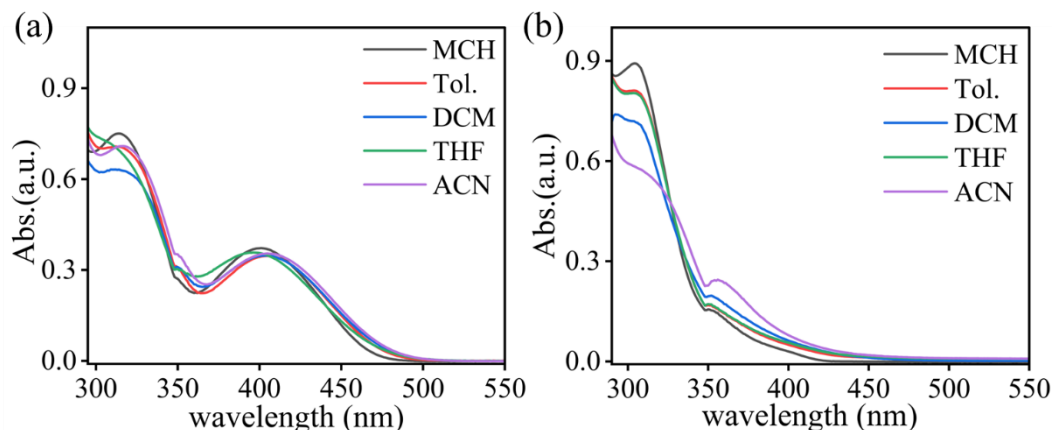


Fig. S7. Absorption spectra of (a) **TPNTZ** and (b) **TPQ TZ** in different solvents at ambient conditions.

S5. Kinetic studies of the thermal back conversion

The Thermal back conversion kinetics from QC→NBD-derivatives were monitored using absorption spectroscopy at different temperatures. Considering a unimolecular back reaction from QC → NBD, the data were analysed according to the first-order kinetics.

$$\frac{d[QC]}{dt} = \frac{d[NBD]}{dt} = k \quad (S5)$$

In eq. S5, [QC] is the concentration of the quadricyclane, [NBD] is the concentration of the norbornadiene, and k is the rate constant of the thermal back reaction at a certain temperature. The rate constant k was obtained by exponential fitting of absorbance at 410 nm. Using the obtained values by fitting in Arrhenius equation (S6) or Eyring equation (S7) rate constant (k) and thermal half-life($t_{1/2}$), entropy and Gibbs free energy at room temperature were calculated.

$$\ln(k) = \ln(A) - \left(\frac{E_a}{R}\right)\left(\frac{1}{T}\right) \quad (S6)$$

$$\ln\left(\frac{k}{T}\right) = \frac{\Delta H^\ddagger}{R} \frac{1}{T} + \ln \frac{k_b}{h} + \frac{\Delta S^\ddagger}{R} \quad (S7)$$

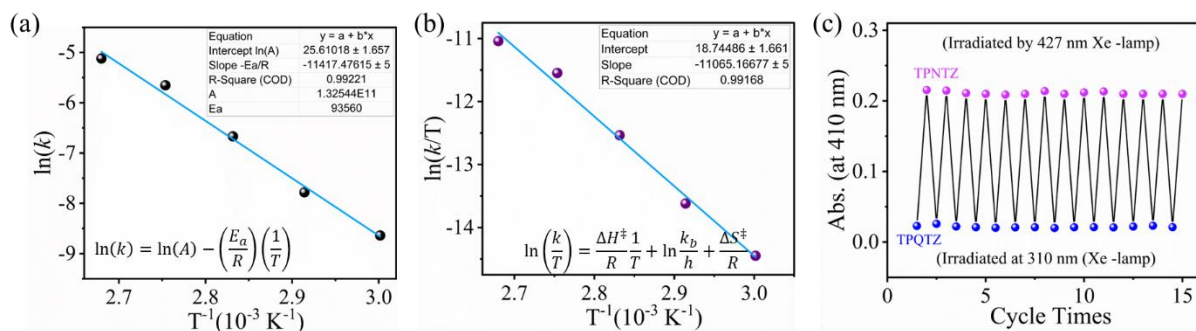


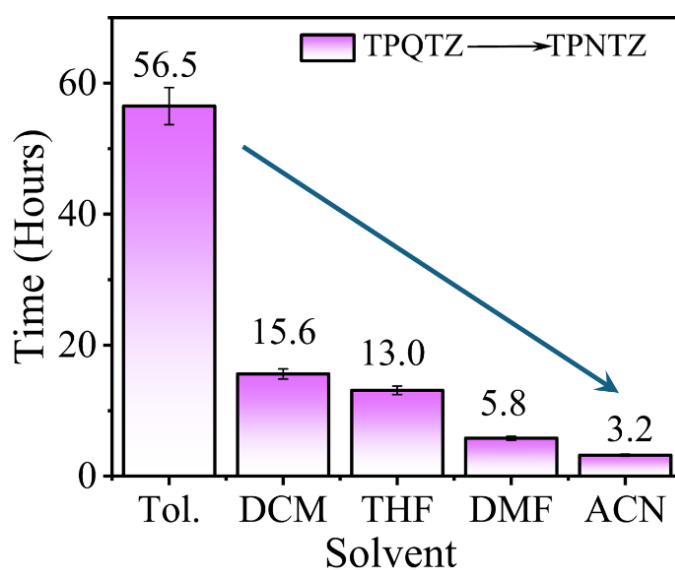
Fig. S8. (a) Arrhenius plot for the conversion of **TPQ TZ**→**TPNTZ**. (b) Eyring plot for the conversion of **TPQ TZ**→**TPNTZ**. (c) Reversible photothermal cycles of **TPNTZ** ⇌ **TPQ TZ** in toluene.

Table S3a. Thermal back conversion kinetics parameter in toluene

Temperature (°C)	100	90	80	70	60
Rate constant k (s ⁻¹)	5.98×10^{-3}	3.51×10^{-3}	1.27×10^{-3}	4.17×10^{-4}	1.77×10^{-4}
Half- life $t_{1/2}$ (s)	115.94	197.55	546.82	1659.87	3917.69

Table S3b. Thermodynamic parameters at RT.

Parameters	TPQTZ → TPNTZ
Activation Energy, E_a (kJ mol ⁻¹)	93.56 ± 3.0
Enthalpy, ΔH^\ddagger (kJ mol ⁻¹)	-91.45 ± 3.0
Entropy, ΔS^\ddagger (JK ⁻¹ mol ⁻¹)	-41.66 ± 2.0
Half-life, $t_{1/2}$ (hours) at 298 K	56.5 ± 1.0
Rate constant, k (s ⁻¹) at 298 K	3.41×10^{-6}

**Fig. S9.** Thermal back-conversion (TPQTZ → TPNTZ) half-life in solvents of varying polarity (Concentration = 10 μ M).

S6. Photoluminescence (PL) studies

Table S4. Solvent-dependent photoluminescence quantum yields (ϕ_{PL}) at ambient conditions.

Solvent	(ϕ_{PL}) in %	
	TPNTZ	TPQTZ
MCH	83.4 \pm 5.0	23 \pm 2.0
Toluene	44.9 \pm 3.0	31.1 \pm 2.0
THF	50.8 \pm 3.0	39.6 \pm 3.5
DCM	58.1 \pm 3.0	26.3 \pm 3.5

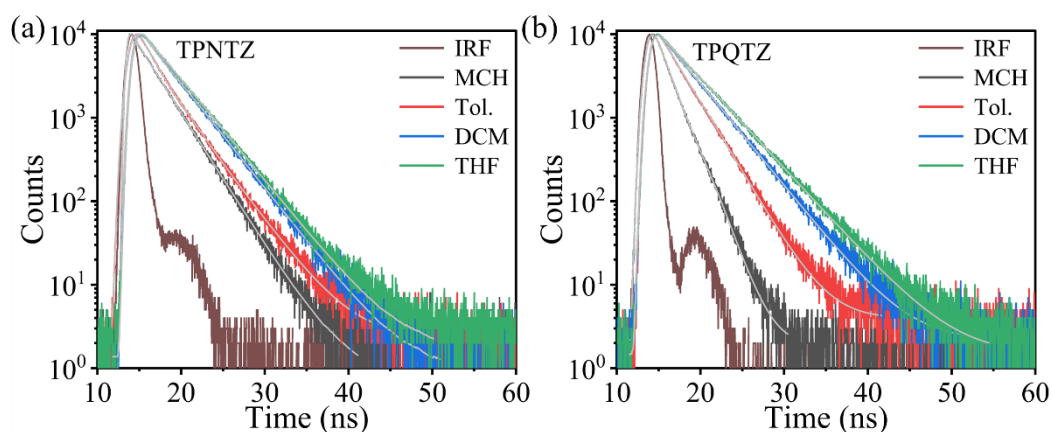


Fig. S10. Fluorescence decays of (a) **TPNTZ** ($\lambda_{\text{ex}} = 410$ nm); and (b) **TPQTZ** ($\lambda_{\text{ex}} = 410$ nm) in different solvents. (Concentration = 10 μM).

Table S5. Solvent-dependent fluorescence lifetimes at ambient conditions

Solvent	TPNTZ ($\lambda_{\text{ex}} = 415$ nm)		TPQTZ ($\lambda_{\text{ex}} = 320$ nm)	
	λ_{em} (nm)	Lifetime (τ , ns)	λ_{em} (nm)	Lifetime (τ , ns)
MCH	556	4.32 ns	445	3.10 ns
Tol	563	4.90 ns	476	5.06 ns
DCM	590	6.27 ns	565	7.20 ns
THF	600	6.74 ns	590	7.35 ns

Lifetimes (τ) are determined from the fitting function of $I(\tau) = Ae^{-t/\tau}$ A is the pre-exponential factors.

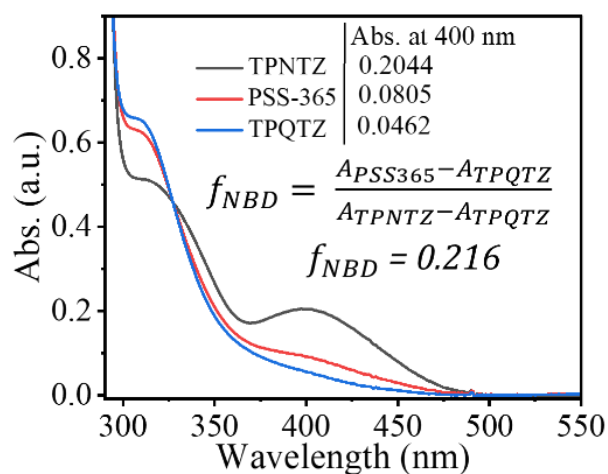


Fig. S11. UV-vis absorption spectra of **TPNTZ**, **PSS-365**, and **TPQTZ** in MCH. Calculated fraction of **TPNTZ** at **PSS-365** found to be 0.216.

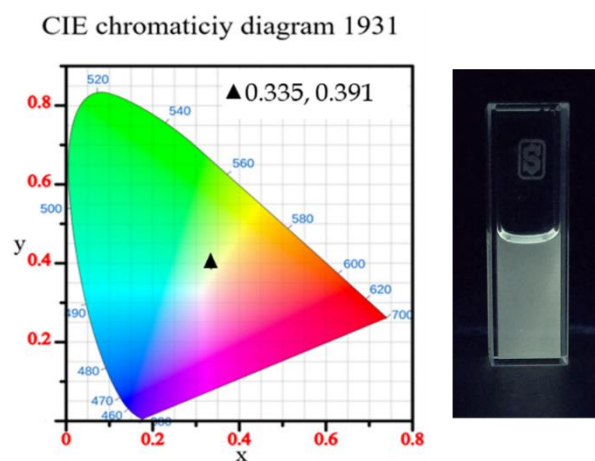


Fig. S12. CIE 1931 chromaticity diagram of **PSS** emission (CIE: 0.335, 0.391) and corresponding fluorescence image under 365 nm UV light in MCH.

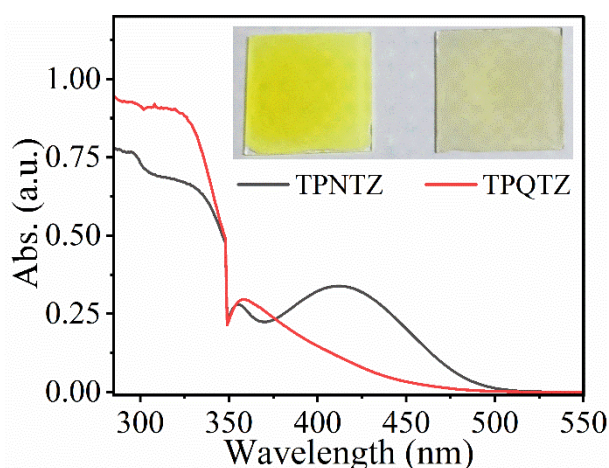


Fig. S13. Absorption spectra of **TPNTZ** and **TPQTZ** film (5 wt% in polystyrene; inset showing digital images of film).

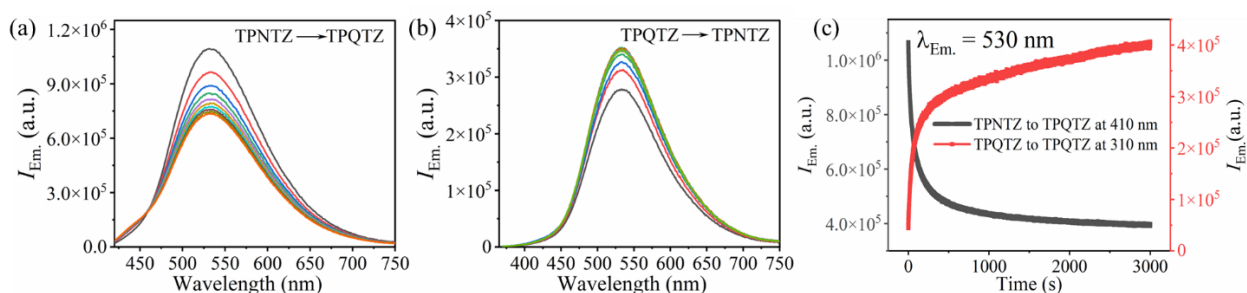


Fig. S14. Emission spectra showing (a) conversion of **TPNTZ** to **TPQ TZ** under 410 nm irradiation; (b) reversion of **TPQ TZ** to **TPNTZ** under 310 nm irradiation; (c) emission intensity at 530 nm versus time, demonstrating reversible switching. (5 wt% in polystyrene film).

S7. Quantum studies.

Density functional theory (DFT) and time-dependent density functional theory (TD-DFT) were performed by employing the meta-GGA functional M06-2X along with the 6-31G(d,p) basis set using the Gaussian package.⁵ Ground-state optimization calculations were performed on geometries from SCXRD analysis or structures drawn in GaussView. Independent gradient model based on Hirshfield partition of molecular density (IGMH) and inter-fragment charge transfer (IFCT) analyses were performed at optimized S1 geometry using multiwfn.⁶

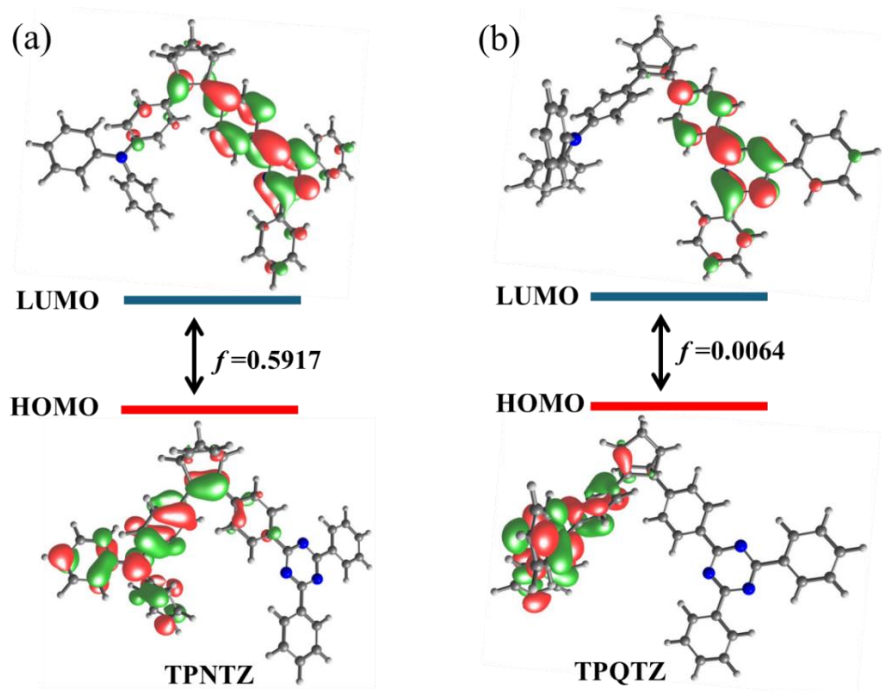


Fig S15. Distribution of frontiers molecular orbitals in (a) **TPNTZ** and (b) **TPQ TZ**. Calculated at M062X/6-31G(d,p) level of theory; isosurface values of ± 0.05 au.

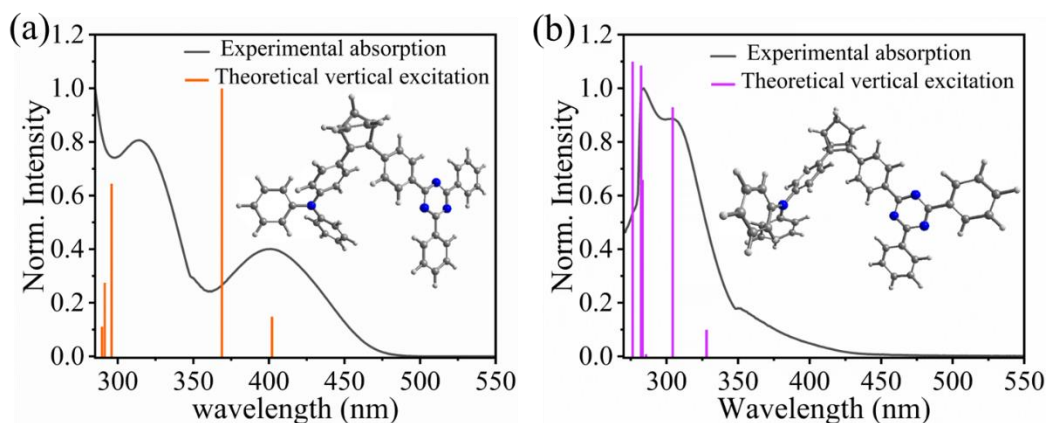
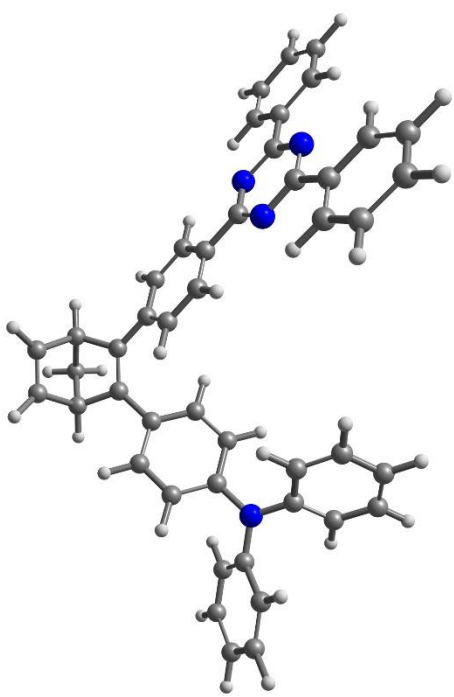


Fig S16. Absorption spectra (in toluene) and calculated excitation spectra (vertical line, gas phase) (a) **TPNTZ** and (b) **TPQTZ**. Calculated at M062X/6-31G(d,p) level of theory.

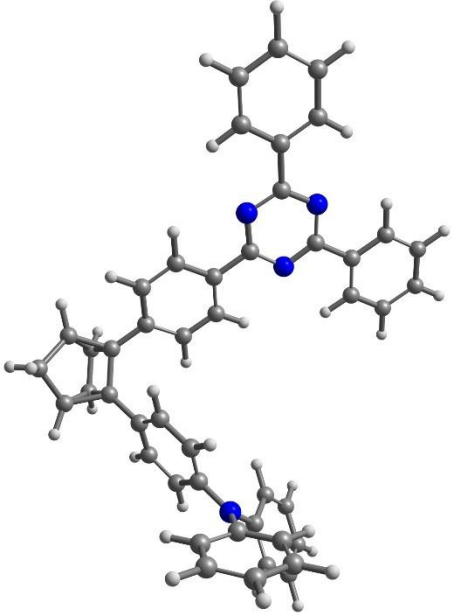
Optimized Coordinates

TPNTZ (C₄₆H₃₄N₄) 	6	-1.487506000	5.520973000	2.265954000
	6	-2.786452000	5.225443000	2.233750000
	6	-3.123879000	4.849381000	0.783321000
	6	-2.363453000	3.544134000	0.456230000
	6	-1.048771000	3.843241000	0.503737000
	6	-0.953050000	5.350340000	0.834419000
	6	-2.192748000	5.849750000	0.053686000
	6	0.129351000	2.968926000	0.425579000
	6	-3.050626000	2.278741000	0.184125000
	6	-4.265402000	1.980934000	0.814862000
	6	-4.926125000	0.781960000	0.583998000
	6	-4.402437000	-0.149670000	-0.319149000
	6	-3.203129000	0.152287000	-0.980910000
	6	-2.540156000	1.341026000	-0.726955000
	6	0.134336000	1.701883000	1.030860000
	6	1.253474000	0.888049000	0.965864000
	6	2.404033000	1.318722000	0.295168000
	6	2.414130000	2.583243000	-0.299924000
	6	1.293275000	3.397954000	-0.228145000
	7	-5.069050000	-1.370018000	-0.566843000
	6	-4.322743000	-2.558912000	-0.759628000

	6	-6.484512000	-1.414743000	-0.598369000
	6	3.596584000	0.445114000	0.218576000
	7	3.535148000	-0.748537000	0.817037000
	6	4.632434000	-1.502670000	0.716869000
	7	5.743747000	-1.136957000	0.071973000
	6	5.710790000	0.073136000	-0.493526000
	7	4.663088000	0.899672000	-0.446940000
	6	6.919967000	0.528657000	-1.223281000
	6	4.615889000	-2.837447000	1.365326000
	6	8.046892000	-0.295079000	-1.297706000
	6	9.177827000	0.133020000	-1.982341000
	6	9.191443000	1.383759000	-2.596175000
	6	8.069765000	2.207176000	-2.523708000
	6	6.936814000	1.783030000	-1.839958000
	6	3.484359000	-3.262327000	2.067622000
	6	3.470884000	-4.512132000	2.674907000
	6	4.584217000	-5.345080000	2.584686000
	6	5.713375000	-4.924569000	1.885070000
	6	5.731435000	-3.675108000	1.277089000
	6	-4.719550000	-3.493851000	-1.722259000
	6	-3.989302000	-4.662815000	-1.901949000
	6	-2.847629000	-4.909260000	-1.143261000
	6	-2.447923000	-3.974974000	-0.190928000
	6	-3.182219000	-2.812220000	0.010574000
	6	-7.210920000	-0.391438000	-1.217790000
	6	-8.599894000	-0.435978000	-1.239025000
	6	-9.283600000	-1.504522000	-0.663833000
	6	-8.560505000	-2.528175000	-0.056603000
	6	-7.171851000	-2.483952000	-0.013237000
	1	-0.878067000	5.772040000	3.124674000
	1	-3.483563000	5.182212000	3.061265000
	1	-4.179750000	4.846955000	0.511053000
	1	0.011198000	5.815658000	0.628721000

	1	-2.125789000	5.668253000	-1.021973000
	1	-2.441485000	6.893324000	0.261457000
	1	-4.685283000	2.688302000	1.524868000
	1	-5.853820000	0.559692000	1.100913000
	1	-2.801222000	-0.554536000	-1.699410000
	1	-1.618947000	1.563826000	-1.256142000
	1	-0.753069000	1.367559000	1.558659000
	1	1.256616000	-0.088231000	1.437034000
	1	3.308196000	2.912618000	-0.816965000
	1	1.309384000	4.375349000	-0.701276000
	1	8.019209000	-1.264966000	-0.814491000
	1	10.050656000	-0.509236000	-2.037717000
	1	10.075564000	1.716468000	-3.130790000
	1	8.078807000	3.181434000	-3.001348000
	1	6.055366000	2.410463000	-1.773999000
	1	2.627289000	-2.601378000	2.127889000
	1	2.591242000	-4.837797000	3.220476000
	1	4.572032000	-6.321069000	3.059539000
	1	6.581211000	-5.572013000	1.813954000
	1	6.601587000	-3.332075000	0.729254000
	1	-5.602120000	-3.295607000	-2.321773000
	1	-4.309218000	-5.378932000	-2.652194000
	1	-2.275338000	-5.818296000	-1.293114000
	1	-1.563038000	-4.155908000	0.410921000
	1	-2.876778000	-2.089372000	0.760102000
	1	-6.677084000	0.434621000	-1.676423000
	1	-9.149928000	0.365201000	-1.722375000
	1	-10.367379000	-1.539166000	-0.689109000
	1	-9.079917000	-3.364333000	0.400662000
	1	-6.608419000	-3.275913000	0.469391000

TPQTZ (C ₄₆ H ₃₄ N ₄)	6	-1.179374000	4.956363000	-2.240129000
	6	-2.680074000	4.634910000	-2.163204000

	6	-3.083194000	5.104159000	-0.790181000
	6	-2.426658000	3.744922000	-0.970345000
	6	-0.903757000	4.076432000	-1.032061000
	6	-0.843193000	5.579049000	-0.907366000
	6	0.210512000	3.127051000	-0.829891000
	6	-3.042697000	2.463838000	-0.570281000
	6	-2.566031000	1.761179000	0.543005000
	6	-3.148678000	0.565073000	0.937008000
	6	-4.247366000	0.048982000	0.239340000
	6	-4.734833000	0.749345000	-0.868553000
	6	-4.124785000	1.929589000	-1.274335000
	6	0.136617000	1.835702000	-1.373222000
	6	1.177042000	0.935406000	-1.206702000
	6	2.324967000	1.306398000	-0.497136000
	6	2.405499000	2.589561000	0.048960000
	6	1.355467000	3.484343000	-0.110438000
	7	-4.850581000	-1.166769000	0.644749000
	6	-5.256974000	-2.111444000	-0.327123000
	6	-5.027203000	-1.440417000	2.022130000
	6	3.441006000	0.348595000	-0.324814000
	7	3.292542000	-0.880694000	-0.827910000
	6	4.325091000	-1.708023000	-0.647320000
	7	5.455255000	-1.378335000	-0.015768000
	6	5.511262000	-0.127884000	0.451213000
	7	4.531629000	0.770259000	0.322992000
	6	6.746272000	0.291553000	1.159260000
	6	4.208908000	-3.086807000	-1.183436000
	6	7.796746000	-0.613715000	1.335176000
	6	8.952553000	-0.218345000	1.997693000
	6	9.067581000	1.080921000	2.487539000
	6	8.022312000	1.985661000	2.313537000
	6	6.864562000	1.594258000	1.652132000
	6	3.039627000	-3.490234000	-1.834703000

	6	2.931963000	-4.782368000	-2.334429000
	6	3.988847000	-5.678490000	-2.188418000
	6	5.155748000	-5.279224000	-1.540065000
	6	5.267327000	-3.988274000	-1.038133000
	6	-6.443338000	-2.835645000	-0.160050000
	6	-6.833049000	-3.767884000	-1.114415000
	6	-6.062682000	-3.980288000	-2.255146000
	6	-4.887454000	-3.252996000	-2.426717000
	6	-4.478542000	-2.332001000	-1.469486000
	6	-5.407537000	-0.420510000	2.902137000
	6	-5.567046000	-0.689632000	4.256310000
	6	-5.369919000	-1.976170000	4.751874000
	6	-5.000047000	-2.993245000	3.875281000
	6	-4.819345000	-2.731171000	2.522387000
	6	-2.095675000	6.113126000	-0.245891000
	1	-0.573996000	5.051658000	-3.131306000
	1	-3.360435000	4.497392000	-2.993734000
	1	-4.134837000	5.113882000	-0.526467000
	1	0.121715000	6.059232000	-0.789560000
	1	-1.713220000	2.149394000	1.092805000
	1	-2.759901000	0.021305000	1.791931000
	1	-5.583180000	0.352372000	-1.416833000
	1	-4.502020000	2.451900000	-2.149212000
	1	-0.750598000	1.544325000	-1.927704000
	1	1.120003000	-0.062588000	-1.625995000
	1	3.293671000	2.868764000	0.604343000
	1	1.416977000	4.472393000	0.334911000
	1	7.690524000	-1.620469000	0.947713000
	1	9.765568000	-0.924174000	2.132639000
	1	9.971217000	1.388165000	3.004499000
	1	8.110539000	2.998003000	2.694051000
	1	6.041930000	2.285151000	1.507416000
	1	2.227008000	-2.780440000	-1.938687000

	1	2.022213000	-5.092078000	-2.838242000
	1	3.903071000	-6.687517000	-2.579171000
	1	5.979597000	-5.976036000	-1.425509000
	1	6.167580000	-3.661295000	-0.530579000
	1	-7.050361000	-2.662577000	0.722616000
	1	-7.754988000	-4.322123000	-0.969451000
	1	-6.374396000	-4.703474000	-3.000955000
	1	-4.272917000	-3.411880000	-3.307230000
	1	-3.556310000	-1.774766000	-1.597912000
	1	-5.571696000	0.579793000	2.514875000
	1	-5.860764000	0.112419000	4.926076000
	1	-5.501977000	-2.183412000	5.808273000
	1	-4.835250000	-3.999393000	4.247615000
	1	-4.518211000	-3.521564000	1.842648000
	1	-2.033692000	6.082214000	0.846179000
	1	-2.327531000	7.134307000	-0.564436000

S8. Supporting References

1. G. M. Sheldrick, *Acta Crystallogr. C: Struct. Chem.*, 2015, **71**, 3-8.
2. O. V. Dolomanov, L. J. Bourhis, R. J. Gildea, J. A. Howard and H. Puschmann, *J. Appl. Crystallogr.*, 2009, **42**, 339-341.
3. (a) N. Acharya, M. Upadhyay, S. Dey and D. Ray, *J. Phys. Chem. C*, 2023, **127**, 7536-7545; (b) S. Dey, A. K. Pal, M. Upadhyay, A. Datta and D. Ray, *J. Phys. Chem. B*, 2023, **127**, 9833-9840.
4. (a) K. Stranius and K. Börjesson, *Scientific reports*, 2017, **7**, 41145; (b) B. Vandekerckhove, N. Piens, B. Metten, C. V. Stevens and T. S. Heugebaert, *Org. Process Res. Dev.*, 2022, **26**, 2392-2402, (c) J. Rabani, H. Mamane, D. Pousty, J. R. Bolton, *Photochem. Photobiol.* 2021, **97**, 873-902. (d) H. J. Kuhn, S. E. Braslavsky, R. Schmidt, *Pure & Appl. Chem.*, 1989, **61**, 187-210.
5. (a) M. J. Frisch, et al., Gaussian 16, Revision C.01. 2016, Gaussian Inc., Wallingford, CT, 2016.; (b) E. G. Hohenstein, S. T. Chill and C. D. Sherrill, *J. Chem. Theory Comput.*, 2008, **4**, 1996-2000.
6. T. Lu and F. Chen, *J. Comput. Chem.*, 2012, **33**, 580-592.